Low-frequency Raman scattering in alkali tellurite glasses

ANGELOS G KALAMPOUNIAS

Department of Chemical Engineering, University of Patras, P.O. Box 1414, GR 26504, Patras, Greece
Also at Foundation for Research and Technology Hellas, Institute of Chemical Engineering and
High Temperature Chemical Processes, FORTH/ICE-HT, Patras, Greece

Abstract. Raman scattering has been employed to study the alkali-cation size dependence and the polarization characteristics of the low-frequency modes for the glass-forming tellurite mixtures, $0.1M_2O–0.9TeO_2$ (M = Na, K, Rb and Cs). The analysis has shown that the Raman coupling coefficient alters by varying the type of the alkali cation. The addition of alkali modifier in the tellurite network leads to the conversion of the TeO_4 units to TeO_3 units with a varying number of non-bridging oxygen atoms. Emphasis has also been given to the low-frequency modes and particular points related to the low-frequency Raman phenomenology are discussed in view of the experimental findings.

Keywords. Tellurites; Raman spectroscopy; alkali tellurite glasses.

1. Introduction

Tellurite glasses have scientific and technological interest due to their attractive physical properties such as low melting points, high dielectric constant (Stanworth 1952; Ulrich 1964), high refractive index (Stanworth 1952) and good infrared transmissivity (Burger *et al* 1985). Compared with silicate and phosphate glasses, tellurites exhibit relatively higher refractive indices, dielectric constants and lower phonon energies. The refractive indices allow the utilization of these glasses for non-linear optical materials (Shioya *et al* 1995) and the phonon energies have atleast two important consequences, the improved infrared transmission up to 6 μm and the low multiphonon decay rates compared to other network oxide glasses. Furthermore, tellurite glasses possess chemical durability and are water resistive (Redman and Chen 1967).

Currently, there exists a large amount of literature regarding the structure of pure TeO_2 and $xM_2O–(1 – x)$ TeO_2 (M: alkali oxide, *x*: mole fraction) glasses with Raman spectroscopy (see e.g. Sekiya *et al* 1992; Tatsumisago *et al* 1994a; Noguera *et al* 2003). However, a limited number of articles have focused on the low-frequency region of the Raman spectra and the comparison between binary glasses with the same concentration in alkali oxide but with different types of cation.

In the present paper, we report the room temperature Raman spectra of the $0.1M_2O–0.9TeO_2$ (M = Na, K, Rb and Cs) glasses. The data are discussed in terms of the glass local structure and the effect of the incorporated cation in the glass. Emphasis has been given in the analysis of the low-frequency Raman features and the relation of the observed data to the cation size.

2. Experimental

The reagent grade chemicals, tellurium (IV) oxide (99.99% purity) and sodium, potassium, rubidium and cesium carbonates (99.95% purity) were purchased from Alfa Aesar. The appropriate amounts of polycrystalline TeO_2 and M_2CO_3 (M = Na, K, Rb and Cs) were mixed and melted in platinum crucibles at 700–800°C for 15–30 min. The homogenized bubble-free liquids were quenched using the conventional method by dipping the crucible into cold water. Heating of the samples was performed at temperatures near the glass transition temperature in order to avoid cracking due to relieved internal stresses generated by quenching.

Raman spectra were recorded using the 514.5 nm line of an Ar^+ laser as excitation source. The laser power at the sample was set at ~ 200 mW. The scattered light was resolved by a triple monochromator/spectrograph Jobin Yvon T64000, set at the double subtractive mode configuration for better stray light rejection and for sharp cutoff of the exciting laser line at low frequencies. The spectral resolution was fixed at 2 cm^{-1}, while the scattered light was detected by a CCD detector. A system of achromatic and anti-reflection coated lenses was used to collect the right angle scattered light. Both polarized (VV: vertical polarization of incident laser–vertical analysis of scattered light) and depolarized (VH: vertical polarization of incident laser–horizontal analysis of scattered light)

(angelos@chemeng.upatras.gr)

scattering geometries were employed for glasses. This was achieved with the aid of a set of Glan and Glan-Thompson polarizers (Hale) with extinction coefficients better than 10^{-6} and 10^{-7}, respectively. A calibration procedure with the aid of a CCl_4 sample was often taking place in order to check the polarization and correct for possible drifts of the monochromator's gratings. Polycrystalline solids were measured with the vertical-unpolarized (VU) configuration. Accumulation times were adjusted to result in a very high signal-to-noise ratio; few minutes depending on the sample temperature were sufficient for this. All room temperature spectra were recorded in a backscattering geometry under a microscope where the excitation laser beam was focused onto the sample by a microscope objective ($50\times/0.55$). Since the spectral conditions are the same for all $0.1M_2O-0.9TeO_2$ (M = Na, K, Rb and Cs) glasses at room temperature, the Raman intensities could be quantitatively correlated within an error of ~5%.

3. Results and discussion

Based on Raman spectroscopic results the structure of pure TeO_2 and tellurium oxide based glasses reveals two basic findings: First, the pure TeO_2 consists of TeO_4 trigonal bipyramids (tbps) in which one equatorial site of the sp^3d hybrid orbitals is occupied by a lone pair of electrons and the other two equatorial and axial sites are occupied by oxygen atoms. Second, the addition of alkali and/or alkaline earth modifiers to pure TeO_2 network causes a change of the Te coordination polyhedron from TeO_4 tbp to TeO_3 trigonal pyramid (tp) in which one of the Te sp^3 hybrid orbitals is occupied by a lone pair of electrons (Sekiya *et al*

1992; Tatsumisago *et al* 1994a; Noguera *et al* 2003). Figure 1 shows the room temperature polarized and depolarized Raman spectra of $0.1Rb_2O-0.9TeO_2$ glass. The spectrum of the corresponding crystal is also shown for comparison. The spectrum of the glass is characterized by three polarized bands at high frequencies, viz. a broad band near 475 cm^{-1}, an intense band at ~670 cm^{-1} and a shoulder band near ~770 cm^{-1}. These bands have been attributed to the bending mode of Te–O–Te or O–Te–O linkages, to stretching modes of the TeO_4 tbp, to stretching mode of the TeO_3 tp units, respectively (Sekiya *et al* 1992; Tatsumisago *et al* 1994b; Noguera *et al* 2003). At lower frequencies the spectrum is dominated by a well resolved asymmetric peak, viz. the Boson peak, and several low-lying vibrational lines centred at ~130 and ~280 cm^{-1}. These bands observed in the low-frequency region are assigned to a bending vibration of TeO_3 tp having two or three NBO atoms (Sekiya *et al* 1992; Tatsumisago *et al* 1994b). The Raman bands of $0.1Rb_2O-0.9TeO_2$ crystal are similar to that observed in paratellurite *a*-TeO_2 crystal
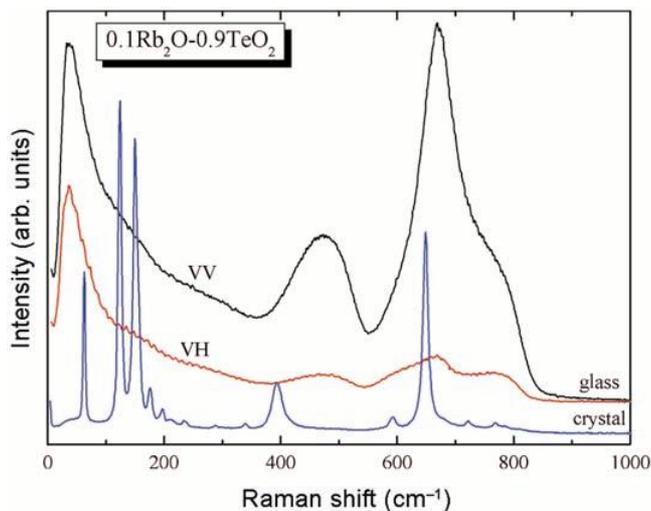
Figure 1. Stokes-side polarized (VV) and depolarized (VH) Raman spectra of $0.1Rb_2O-0.9TeO_2$ glass at room temperature. The spectrum of the corresponding crystal is also shown for comparison (Spectral conditions: excitation line: 514.5 nm, laser power: 200 mW, resolution: 2 cm^{-1}, CCD detector).
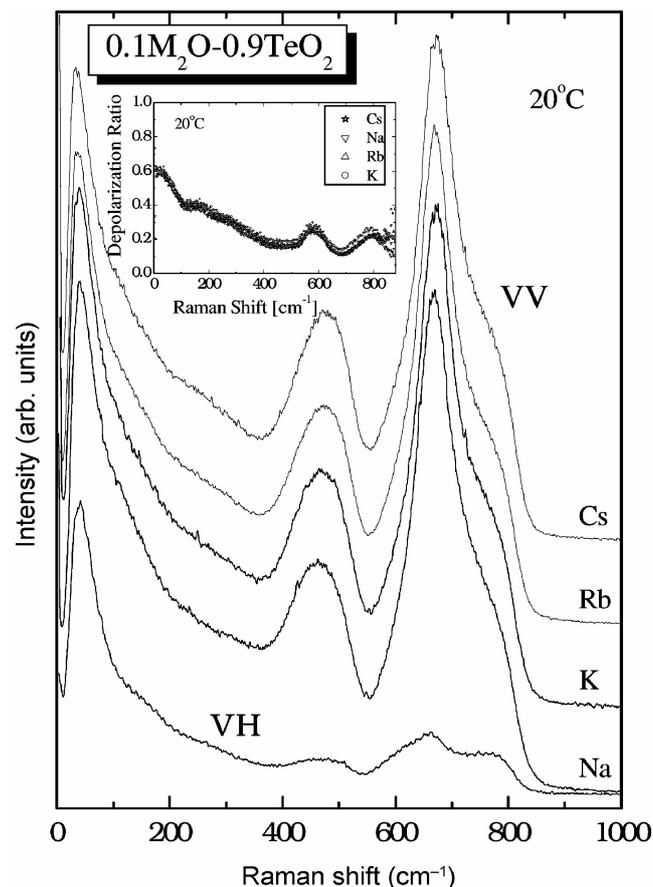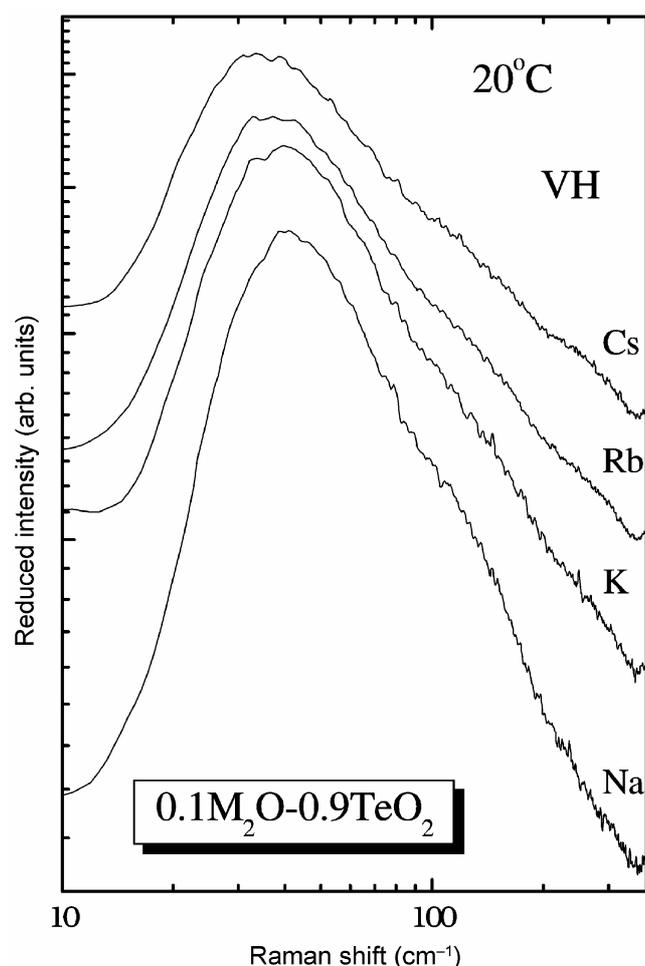

Figure 2. Stokes-side VV Raman spectra of $0.1M_2O-0.9TeO_2$ (M = Na, K, Rb and Cs) glasses at room temperature. The depolarized spectrum is shown only for Na containing glass, inset: depolarization ratio for all glasses at room temperature for comparison (Spectral conditions: excitation line: 514.5 nm, laser power: 400 mW, resolution: 2 cm^{-1}, CCD detector).

(Pine and Dresselhaus 1972). In the paratellurite lattice, the lone pairs of Te-atoms are always oriented vis-á-vis and the two neighbouring TeO_4 tbps, also known as disphenoids, are interconnected via a corner forming a three-dimensional network structure. A comparison of the Raman spectra of the glass and of the corresponding crystal reveals that their structure is not similar.

Figure 2 shows the room temperature polarized Raman spectra of $0 \cdot 1M_2O$–$0 \cdot 9TeO_2$ glasses where M = Na, K, Rb and Cs. The depolarized spectra were measured for all systems but only Na containing glass depolarized spectrum is shown here. The inset of figure 2 illustrates the depolarization ratios for all glasses at room temperature. It seems that the polarization characteristics are similar for all glasses containing different types of alkali.

The low-frequency region (below 150 cm^{-1}) of the Raman spectra of alkali tellurite glasses consists of two contributions. Firstly, the Boson peak, an asymmetric intense peak, which is absent from the spectra of the cor-responding crystals. The nature and origin of this spectral characteristic of amorphous materials have received considerable attention. Secondly, there is the quasielastic (QE) line that appears in the spectrum as a zero centred line with a half width at half height of about 10–15 cm^{-1}. It is usually assigned to a fast relaxation process with characteristic time in the sub-picosecond time scale. In an effort to elucidate the microscopic origin of the Boson peak, its spectral features such as peak frequency, polarization characteristics and intensity have to be studied in detail as a function of some external parameter. In the present study, this is attempted by varying the type of modification i.e. the kind of alkali modifier. The low-frequency Raman spectra, for the series of glasses studied

Figure 3. Stokes-side, low-frequency reduced Raman spectra of $0 \cdot 1M_2O$–$0 \cdot 9TeO_2$ (M = Na, K, Rb and Cs) glasses for VH scattering geometry at room temperature in a log–log representation.
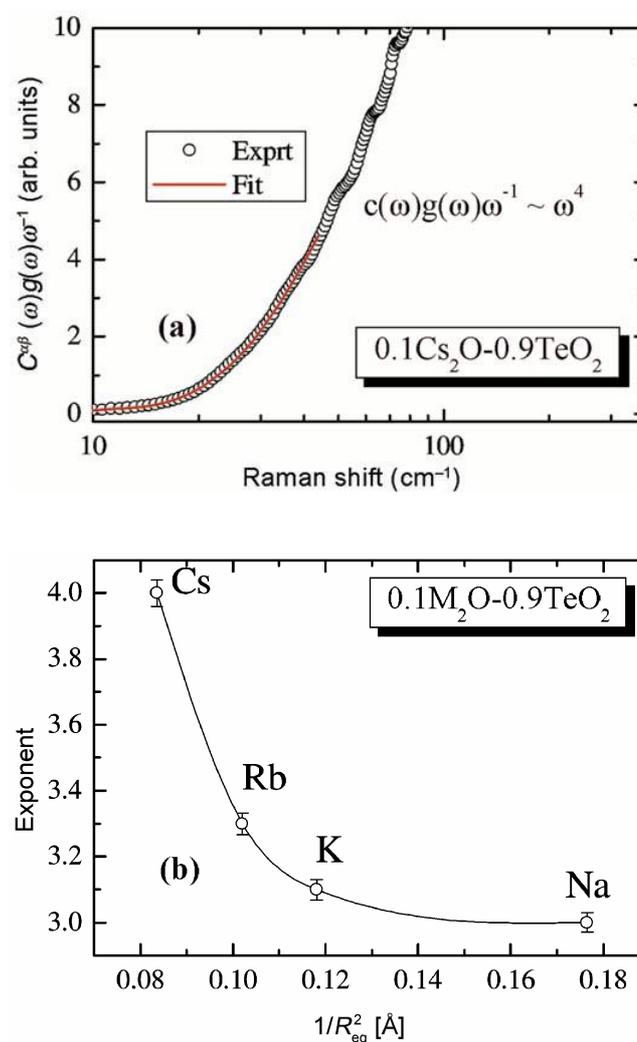
Figure 4. (**a**) Representative semi-logarithmic plot of the reduced depolarized Raman spectra (open circles) for $0 \cdot 1Cs_2O$–$0 \cdot 9TeO_2$ glass. The solid line represents power law fit to the data as described in the text and (**b**) exponent of power law vs $1/\sqrt{R_{eq}^2}$ of alkali cations for $0 \cdot 1M_2O$–$0 \cdot 9TeO_2$ (M = Na, K, Rb and Cs) glasses at room temperature. Solid line is drawn as guide to the eye.

here are shown in figure 3. The spectra are presented in the reduced representation, i.e.

$$I^{red}(\omega) = I^{expt}(\omega)/\omega\,[n(\omega, T)+1] = g(\omega)C^{\alpha\beta}(\omega)/\omega^2,$$

where $g(\omega)$ is the vibrational density of states (VDoS), $C^{\alpha\beta}(\omega)$ the Raman coupling coefficient and $n(\omega, T)$ the Bose–Einstein occupation number. The different components labeled, $\alpha\beta$, denote particular polarization geometries (VV and VH).

The spectrum is generally believed to arise from a breakdown in the Raman selection rule in the disordered material allowing essentially all vibrational modes to participate in the scattering process. This fact led to the conclusion that the Raman scattering is first-order scattering and is closely related to the density of states. In order to isolate the function, $g(\omega)$, the expression

$$I^{\alpha\beta}_{red}(\omega) = \frac{I^{\alpha\beta}(\omega)}{\omega^{-1}[n(\omega,T)+1]} = C^{\alpha\beta}(\omega)g(\omega),$$

is frequently used. The frequency dependence of the coupling coefficient cannot be determined through a direct comparison of Raman and neutron scattering data without taking account for the polarization dependence of $C^{\alpha\beta}(\omega)$. In many studies the Raman coupling coefficient was determined by considering only the depolarized reduced Raman intensity. Detailed analysis of the depolarization ratio for several oxides and chlorides in a wide temperature range showed strong frequency dependence (Papatheodorou and Yannopoulas 2002). $C^{\alpha\beta}(\omega)$ is a very specific property of the studied system related to the way that vibrational motion modulates the polarizability of the medium and as such differs among various liquids. Figure 4(a) shows the frequency dependence of the $C^{\alpha\beta}(\omega)g(\omega)\omega^{-1}$ factor in the low-frequency region (< 100 cm^{-1}) for the

room temperature $0.1Cs_2O$–$0.9TeO_2$ glass. Similar results have been obtained for all $0.1M_2O$–$0.9TeO_2$ glasses. The factor, $C^{\alpha\beta}(\omega)g(\omega)$, has been multiplied by ω^{-1} in order not to suppress the low frequencies. This figure reveals the following facts. First, the limiting low-frequency spectra do not show remnants of the QE component suggesting that it is rather a symmetric line. Second, the frequency dependence of the Raman coupling coefficient can be elucidated. Indeed, the equation

$$C^{\alpha\beta}(\omega)g(\omega)\omega^{-1} \propto \omega^x,$$

is valid as shown in figure 4(a).

Using this power law proportionality in the above equation we obtained the overall exponent, x. The results are shown in figure 4(b) for all $0.1M_2O$–$0.9TeO_2$ glasses at room temperature. It is noteworthy that the resultant values for the power law exponent vary from 4 to 3, depending on the cation. Accordingly, the exponent for the net $C^{\alpha\beta}(\omega)g(\omega)$ product assumes mean values close to 5, 4.3, 4.1 and 4 for Cs, Rb, K and Na, respectively. In the context of the rigid conception at such very low frequencies the vibrational density of states follows fairly well the Debye law, i.e. $g(\omega) \propto \omega^2$. Then, the low frequency behaviour of the Raman coupling coefficient follows a power law with exponents close to 3, 2.3, 2.1 and 2 for Cs, Rb, K and Na, respectively.

In many oxide glasses, as also in the case of tellurite glasses, the presence of low-lying vibrational modes obstructs the quantitative analysis of the BP. In order to overcome this problem we have performed a simple deconvolution procedure on the low-frequency Raman spectra using the fewest possible adjustable parameters. The BP is described with a log-normal distribution, the simplest asymmetric distribution and the low-lying vibrations as Gaussian distributions.

The alkali modifier dependence of the BP is evident in figure 3. As regards the frequency of the BP there is a clear dependence on the square root of the alkali mass as figure 5 reveals. The larger the size of the modifier, the lower the frequency of the BP. This is reasonable considering that modifying cations participate in the vibrating 'structural unit' in the glass that gives rise to the BP. The creation of a larger number of TeO$_3$ tps in the sequence Na $\rightarrow$ Cs is also in agreement with the cation size dependence of the BP frequency. Similar behaviour exhibits the Boson peak frequency in the alkali metaphosphate glasses where also exist some dependence of the cation on the low-frequency scattering (Miller 1979). Further, the depolarization ratio of the various glasses is frequency dependent over the spectral range of the BP exhibiting a clear systematic decrease (see inset in figure 2).
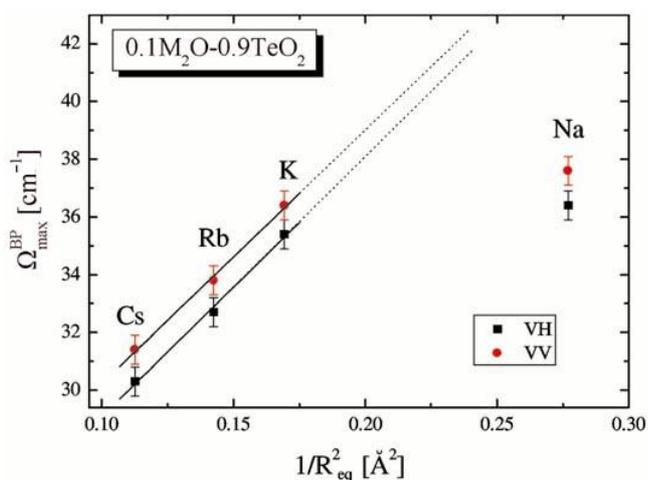
Figure 5. Frequency of the Boson peak maximum vs $1/\sqrt{R_{eq}^2}$ of alkali cations for $0.1M_2O$–$0.9TeO_2$ (M = Na, K, Rb and Cs) glasses at room temperature and VV, VH scattering geometries. Solid lines are drawn as guide to the eye.

4. Conclusions

In this paper we present the Raman spectra of $0.1M_2O$–$0.9TeO_2$ (M = Na, K, Rb and Cs) alkali tellurite glasses in

an effort to elucidate the changes caused in the low frequency behaviour of the Raman coupling coefficient by altering the type of the alkali cation. The network structure of the tellurite glass is composed of TeO_4 trigonal bipyramid and TeO_3 trigonal pyramid units. On adding alkali modifier in the network, the TeO_4 units are converted to TeO_3 units with a varying number of non-bridging oxygen atoms. The low-frequency Raman spectral features reveal cation dependence as in the case of alkali metaphosphate glasses. The dependence of the maximum of the Boson peak as a function of cation size has also been determined and the results reveal a monotonic decrease.

Acknowledgements

References

Burger H, Vogel W and Kozhukharov V 1985 *Infrared Phys.* **25** 395

Miller Ph J 1979 *J. Chem. Phys.* **71** 997

Noguera O, Merle-Mejean T, Mirgorodsky A P, Smirov M B, Thomas P and Champarnaud-Mesjard J-C 2003 *J. Non-Cryst. Solids* **330** 50

Papatheodorou G N and Yannopoulos S N 2002 *Molten salts: From fundamentals to applications* (ed.) M Gaune-Escard (Dordrecht: Kluwer Academic) pp 47–106

Pine A S and Dresselhaus G 1972 *Phys. Rev.* **B5** 4087

Redman M J and Chen J H 1967 *J. Am. Ceram. Soc.* **50** 523

Sekiya T, Mochida N, Ohtsuka A and Tonokawa M 1992 *J. Non-Cryst. Solids* **144** 128

Shioya K, Kmatsu T, Kim H G, Sato R and Matsusita K 1995 *J. Non-Cryst. Solids* **189** 16

Stanworth J E 1952 *Nature* **169** 581

Tatsumisago M, Minami T, Kowada Y and Adashi H 1994a *Phys. Chem. Glasses* **35** 89

Tatsumisago M, Lee S-K, Minami T and Kowada Y 1994b *J. Non-Cryst. Solids* **177** 154

Ulrich D R 1964 *J. Am. Ceram. Soc.* **47** 595